CARDIFF UNIVERSITY
PRIFYSGOL CAERDYDD

ORCA – Online Research @ Cardiff

This is an Open Access document downloaded from ORCA, Cardiff University's institutional repository:https://orca.cardiff.ac.uk/id/eprint/144575/

This is the author's version of a work that was submitted to / accepted for publication.

Citation for final published version:

Jia, Zhiyong, Rondiya, Sachin R., Cross, Russell W., Wang, Cheng, Dzade, Nelson Y. and Zhang, Chuang 2021. Highly active methanol oxidation electrocatalyst based on 2D NiO porous nanosheets:a combined computational and experimental study. Electrochimica Acta 394 , 139143. 10.1016/j.electacta.2021.139143

Publishers page: http://dx.doi.org/10.1016/j.electacta.2021.139143

Please note:
Changes made as a result of publishing processes such as copy-editing, formatting and page numbers may not be reflected in this version. For the definitive version of this publication, please refer to the published source. You are advised to consult the publisher's version if you wish to cite this paper.

This version is being made available in accordance with publisher policies. See http://orca.cf.ac.uk/policies.html for usage policies. Copyright and moral rights for publications made available in ORCA are retained by the copyright holders.

Highly Active Methanol Oxidation Electrocatalyst based on 2D NiO Porous Nanosheets: A Combined Computational and Experimental Study

ZhiyongJia[a]; Sachin R. Rondiya[b]; Russell W. Cross[b]; Cheng Wang [c]; Nelson Y. Dzade[b]*;

Chuang Zhang[a,c]*

[a] School of Automobile and Traffic Engineering, Hubei University of Arts and Science, Xiangyang 441058, P. R. China.

[b]School of Chemistry, Cardiff University, Main Building, Park Place, Cardiff, CF103AT, Wales, United Kingdom.

[c] Zhang Jiagang Joint Institute for Hydrogen Energy and Lithium-Ion Battery Technology, INET, Tsinghua University, Beijing 100000, P. R. China.

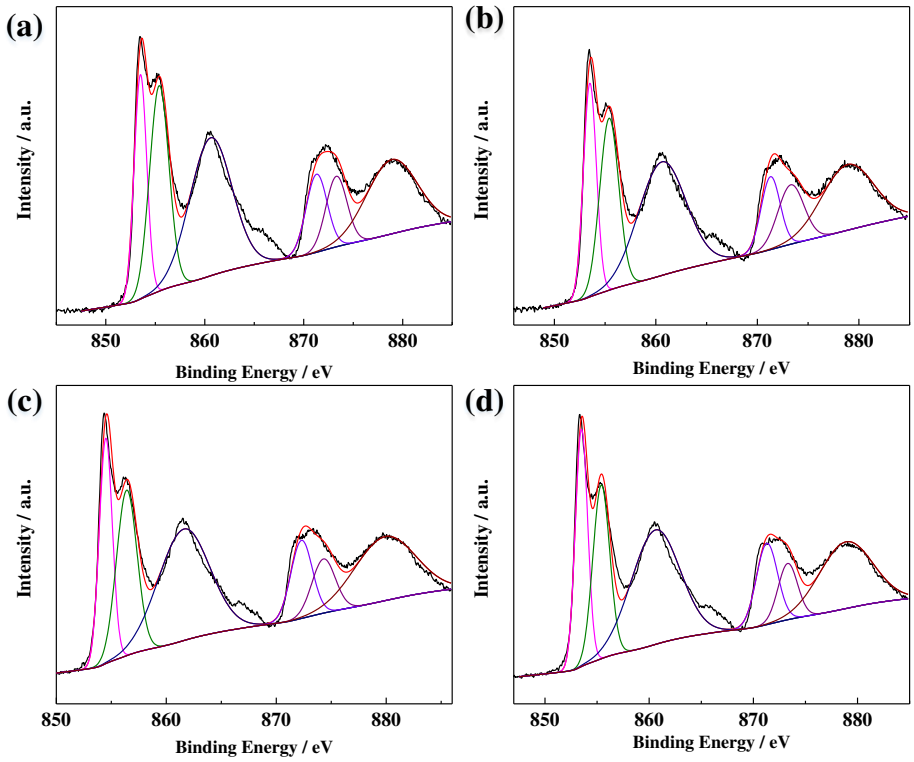

Fig.S1:Ni 2pXPS spectra of the 350-NiO (a), 450-NiO (b), 550-NiO (c) and650-NiO.

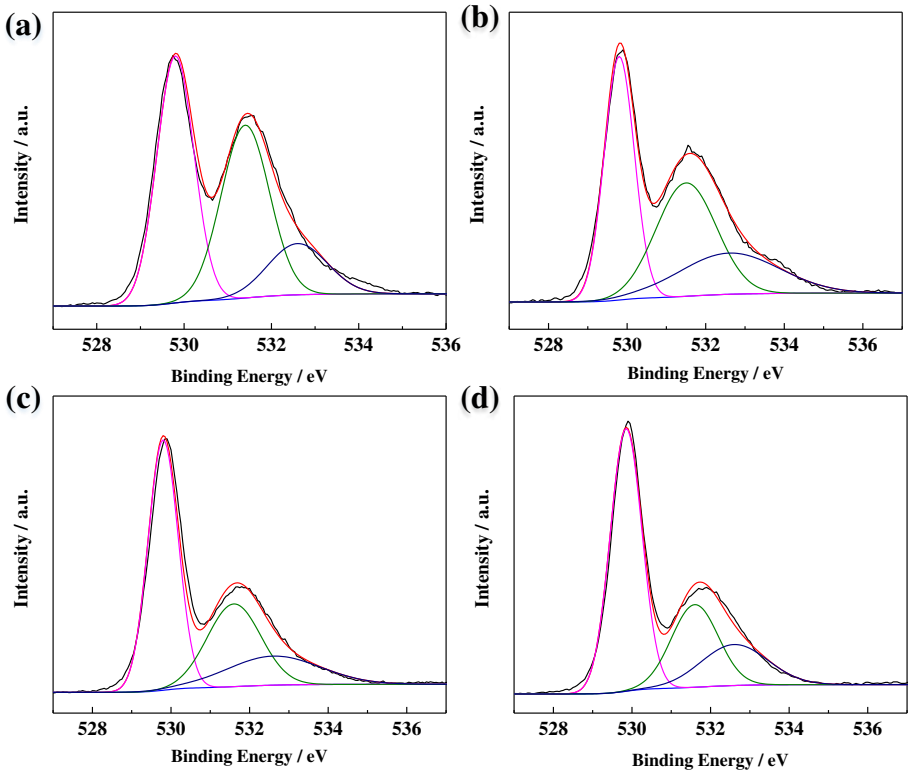

Fig.S2:O 1sXPS spectra of 350-NiO (a), 450-NiO (b), 550-NiO (c) and650-NiO.

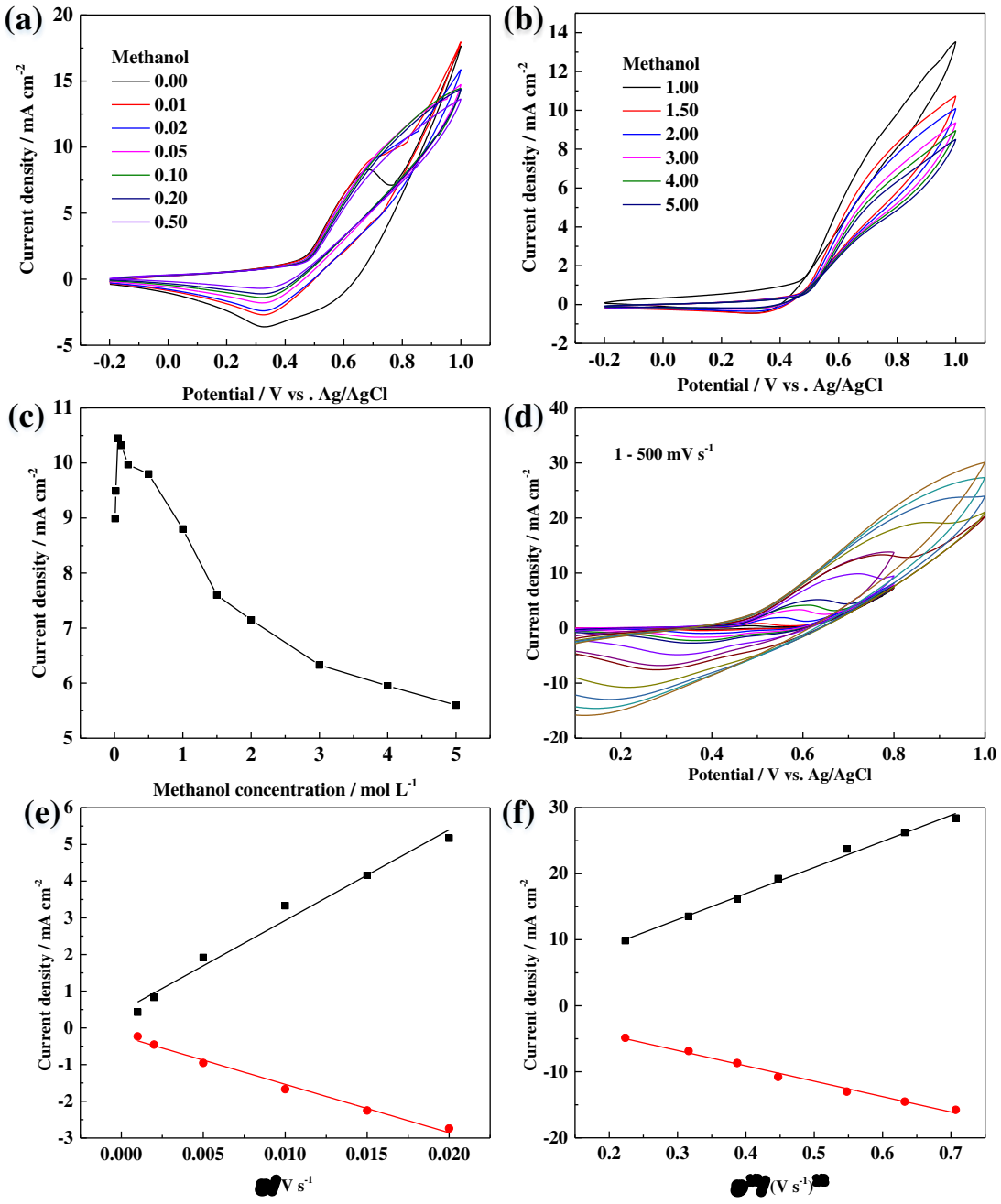

Fig.S3:350-NiO. (a) and (b) CV curves under different methanol concentration at 50 mV s^{-1}, (c) comparison of oxidation peaks of methanol at different concentrations; (d) CV curves at different scan rates (1, 2, 5, 10, 15, 20, 50, 100, 150, 200, 300, 400, 500), (e) relationship of current densities of oxidation and reduction peaks at low sweep speed (1, 2, 5, 10, 15 and 20 mV s^{-1}), (f) relationship of current densities of oxidation and reduction peaks at higher sweep speed (50, 100, 150, 200, 300, 400 and 500 mV s^{-1}); under the 0.1 M KOH solution in the N_2-saturated.

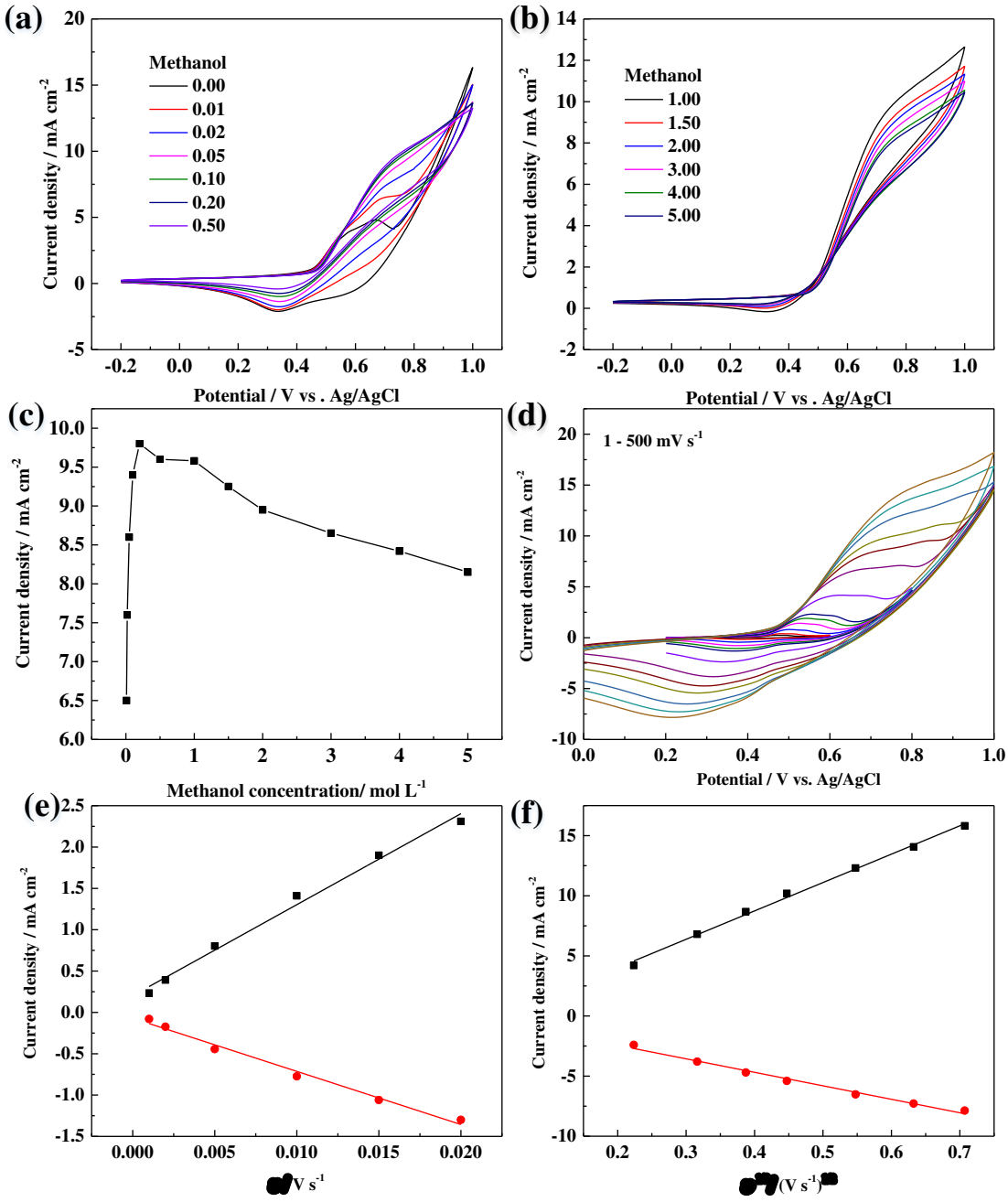

Fig.S4:450-NiO. (a) and (b) CV curves under different methanol concentration at 50 mV s^{-1}, (c) comparison of oxidation peaks of methanol at different concentrations; (d) CV curves at different scan rates (1, 2, 5, 10, 15, 20, 50, 100, 150, 200, 300, 400, 500), (e) relationship of current densities of oxidation and reduction peaks at low sweep speed (1, 2, 5, 10, 15 and 20 mV s^{-1}), (f) relationship of current densities of oxidation and reduction peaks at higher sweep speed (50, 100, 150, 200, 300, 400 and 500 mV s^{-1}); under the 0.1 M KOH solution in the N_2-saturated.

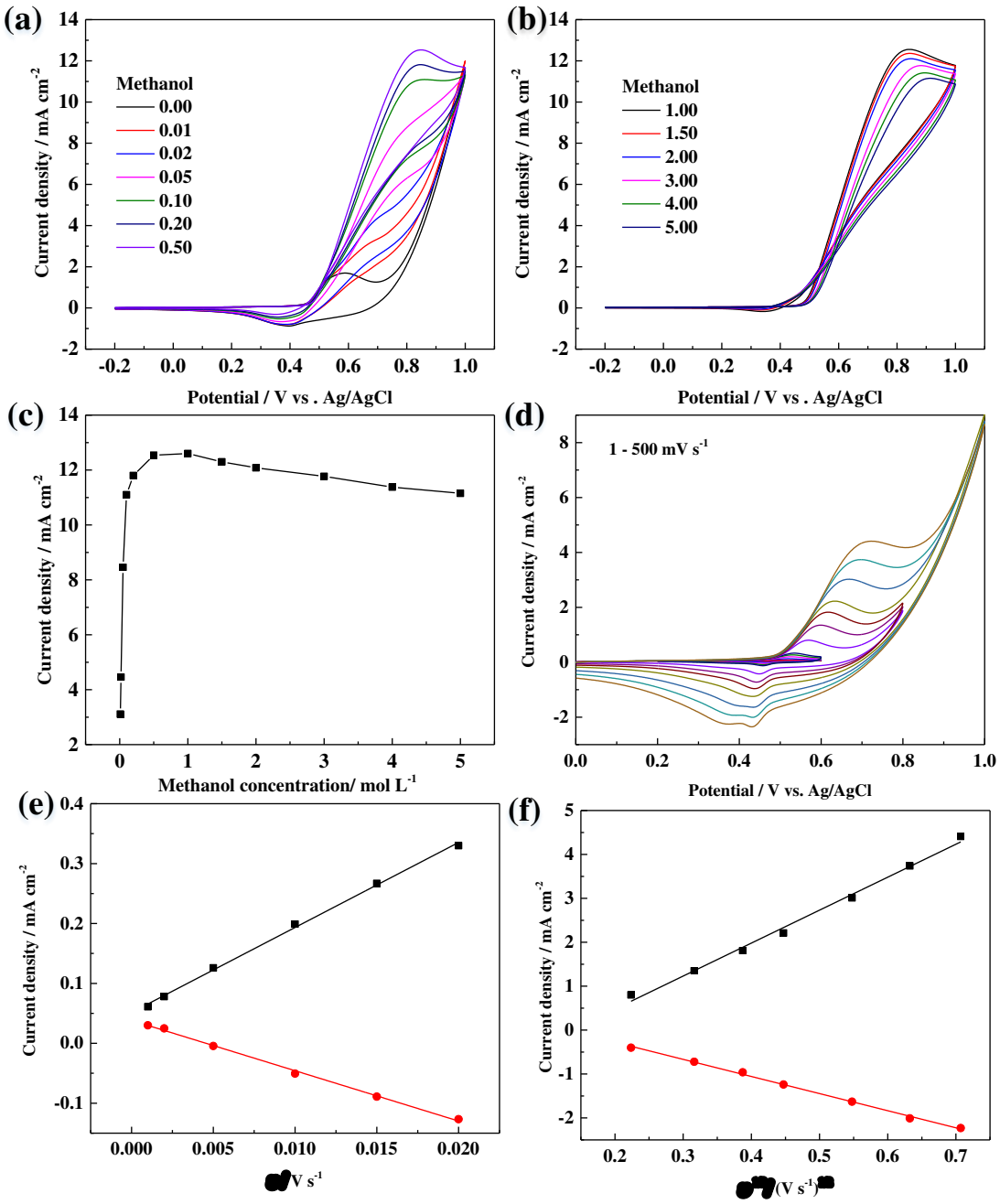

Fig.S5:550-NiO. (a) and (b) CV curves under different methanol concentration at 50 mV s^{-1}, (c) comparison of oxidation peaks of methanol at different concentrations; (d) CV curves at different scan rates (1, 2, 5, 10, 15, 20, 50, 100, 150, 200, 300, 400, 500), (e) relationship of current densities of oxidation and reduction peaks at low sweep speed (1, 2, 5, 10, 15 and 20 mV s^{-1}), (f) relationship of current densities of oxidation and reduction peaks at higher sweep speed (50, 100, 150, 200, 300, 400 and 500 mV s^{-1}); under the 0.1 M KOH solution in the N_2-saturated.

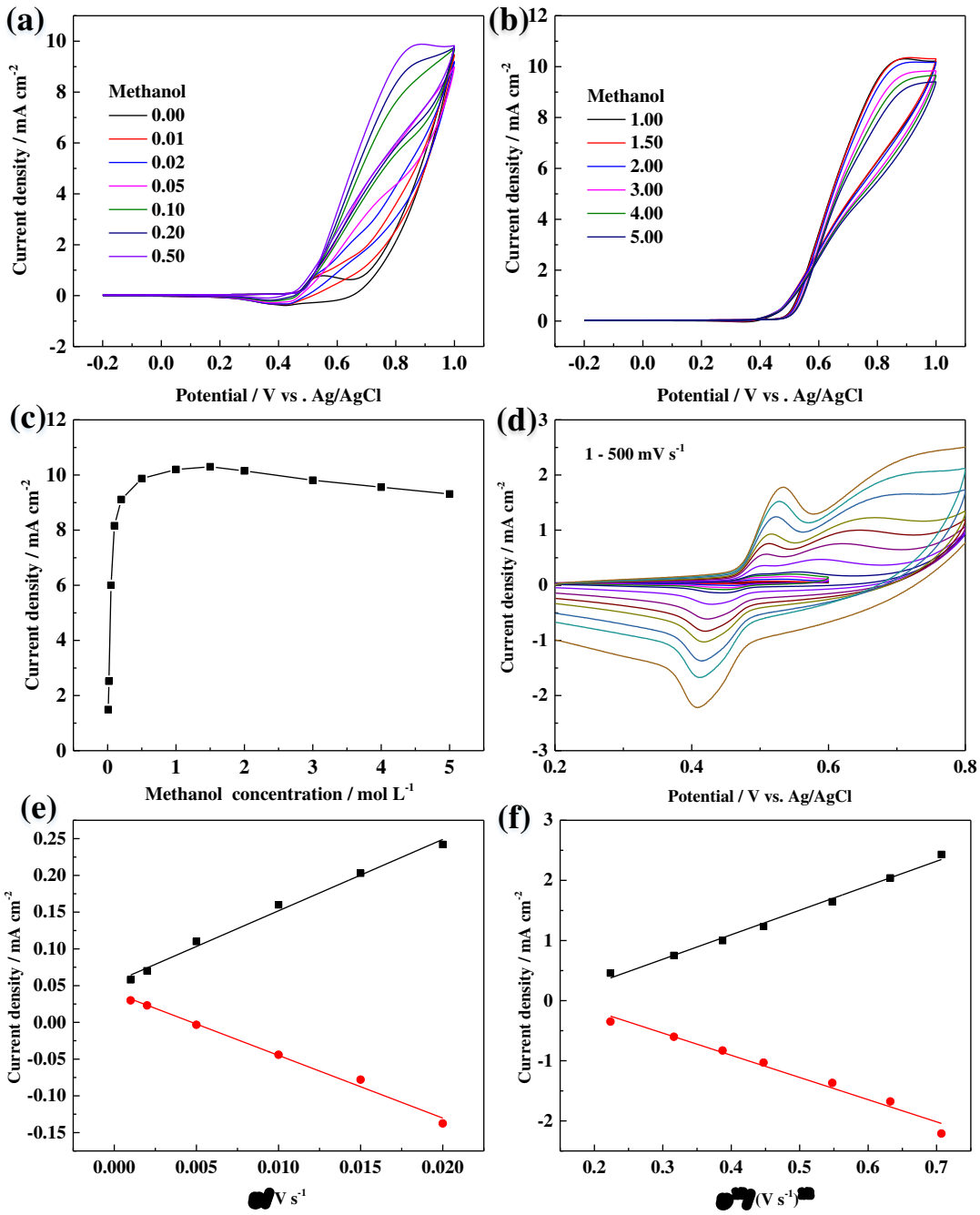

Fig.S6:650-NiO. (a) and (b) CV curves under different methanol concentration at 50 mV s^{-1}, (c) comparison of oxidation peaks of methanol at different concentrations; (d) CV curves at different scan rates (1, 2, 5, 10, 15, 20, 50, 100, 150, 200, 300, 400, 500), (e) relationship of current densities of oxidation and reduction peaks at low sweep speed (1, 2, 5, 10, 15 and 20 mV s^{-1}), (f) relationship of current densities of oxidation and reduction peaks at higher sweep speed (50, 100, 150, 200, 300, 400 and 500 mV s^{-1}); under the 0.1 M KOH solution in the N_2-saturated.

Table S1: Adsorption sites, configurations, energies, and structural parameters for intermediates involved in CH_3OH oxidation on NiO(100).

species	site	configurations	E_{ads} (eV)	d_{C-O} (Å)	d_{Ni-O} (Å)	d_{Ni-C} (Å)
CH_3OH	Ni-top	η^1(O)	−2.14	1.447	2.011	
CH_3O	Ni-top	η^1(O)	−2.42	1.411	1.744	
CH_2OH	Ni_2-top	η^2(C, O)	−2.25	1.456	2.019	1.937
CH_2O	Ni_2-top	η^2(C, O)	−1.70	1.326	1.836	1.978
CHO	Ni_2-top	η^2(C, O)	−3.79	1.251	1.870	1.809
CO	Ni_2-bridge	η^1(C)	−4.20	1.176		1.867, 1.734
HCOOH	Ni_2-top	η^3(C, O, O)	−2.85	1.266, 1.402	1.889, 2.075	2.122
COOH	Ni_2-top	η^2(C, O)	−2.33	1.268, 1.334	1.908	1.851
HCOO	Ni_2-top	η^2(O, O)	−1.88	1.270, 1.275	1.869, 1.914	
CO_2	Ni_2-top	η^2(C, O)	−2.18	1.277, 1.213	1.893	1.919
H_2O	Ni-top	η^1(O)	−1.20		2.015	
OH	Ni_2-bridge	η^1(O)	−4.54		1.934, 1.939	
H	O-top	η^1(H)	−1.19			

Table S2: Reaction energies (ΔE), activation energy barriers (E_a) for the elementary steps involved in the methanol oxidation on NiO(100)

Reactions	ΔE (eV)	E_a(eV)
$CH_3OH \rightarrow CH_2OH + H$	−0.05	0.86
$CH_3OH \rightarrow CH_3O + H$	−0.27	0.54
$CH_3O \rightarrow CH_2O + H$	−1.27	0.90
$CH_2O \rightarrow CHO + H$	−1.05	0.84
$CHO \rightarrow CO + H$	−1.24	0.73
$CHO + OH \rightarrow HCOOH$	+0.19	0.58
$HCOOH \rightarrow COOH + H$	−0.79	0.72
$COOH \rightarrow CO_2 + 2H$	−0.31	0.68
$HCOOH \rightarrow HCOO + H$	−1.21	1.16
$HCOO \rightarrow CO_2 + 2H$	+1.13	0.97